THE JOURNAL OF PHYSICAL CHEMISTRY C

Article

pubs.acs.org/JPCC

Nanolevitation Phenomena in Real Plane-Parallel Systems Due to the Balance between Casimir and Gravity Forces

Victoria Esteso, Sol Carretero-Palacios,* and Hernán Míguez*

Multifunctional Optical Materials Group, Instituto de Ciencia de Materiales de Sevilla (Consejo Superior de Investigaciones Científicas Universidad de Sevilla), Calle Américo Vespucio 49, 41092 Sevilla, Spain

Supporting Information

ABSTRACT: We report on the theoretical analysis of equilibrium distances in real plane-parallel systems under the influence of Casimir and gravity forces at thermal equilibrium. Due to the balance between these forces, thin films of Teflon, silica, or polystyrene in a single-layer configuration and immersed in glycerol stand over a silicon substrate at certain stable or unstable positions depending on the material and the slab thickness. Hybrid systems containing silica and polystyrene, materials which display Casimir forces and equilibrium distances of opposite nature when considered individually, are analyzed in either bilayer arrangements or as composite systems made of a homogeneous matrix with small inclusions inside. For each configuration, equilibrium distances and their stability can be adjusted by fine-tuning of the volume occupied by each material. We find the specific conditions under which nanolevitation of realistic films should be observed. Our results indicate that thin films of real materials in plane-parallel configurations can be used to control suspension or stiction phenomena at the nanoscale.

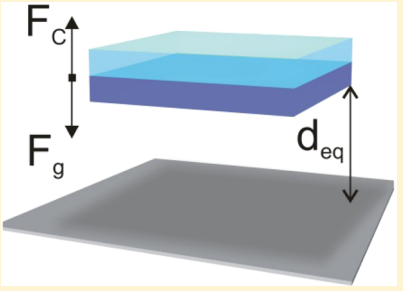

1. INTRODUCTION

Quantum theory states that, at zero temperature and in the absence of any radiation, there are fluctuations of the electromagnetic field (the so-called vacuum fluctuations) that give rise to the well-known van der Waals[1] and Casimir[2] forces between polarizable objects. These forces are at the heart of many fluctuation-induced interactions in biology, chemistry, and physics, being responsible for superlubricity,[3] adhesion,[4,5] and stiction in micro- and nanoelectromechanical (MEM and NEM) devices.[6,7] In particular, the Casimir force[2] was first derived by H. Casimir in 1948, establishing that two perfectly conducting plates in vacuum at zero temperature would be attracted by a force (per unit area A) $F_0 = -(\hbar c\pi^2)/(240d_0^4)$, with d_0 being the separation distance. Later, E. Lifshitz and co-workers[1,8] generalized this prediction and extended it to nonplanar complex geometries containing bodies with arbitrary optical properties at thermal equilibrium. Since then, Lifshitz's theory has been experimentally and theoretically applied to a broad range of conditions covering different length scales,[9] real dielectric materials[10−12] (with rough surfaces[13] or with fluids between the bodies[14]), and diverse geometries (planar,[15] nonplanar,[16] multilayered,[17−19] and corrugated geometries[20,21]). In the same context, the dynamical Casimir effect,[22] induced torques,[23−25] and the response out of thermal equilibrium[26] have been widely investigated as well.

One of the most exceptional predictions of the generalized Lifshitz's theory is the appearance of repulsive Casimir forces[1,7,27−35] when real materials are considered. In particular, in plane-parallel systems the nature of these forces is dictated by the dielectric permittivity of all the objects composing the system through the Fresnel coefficients. Intense repulsive forces are desirable for minimizing friction, adhesion, or stiction in different systems, including MEM and NEM devices. One way to obtain repulsive Casimir forces consists of immersing two objects (characterized by $\varepsilon^{(-1)}(i\xi_n)$ and $\varepsilon^{(1)}(i\xi_n)$, respectively) in a fluid (with $\varepsilon^{(0)}(i\xi_n)$), which satisfy over a wide frequency range the condition $\varepsilon^{(-1)}(i\xi_n) < \varepsilon^{(0)}(i\xi_n) < \varepsilon^{(1)}(i\xi_n)$.[1,28] In the inequation, $\varepsilon(i\xi_n)$ are the dielectric permittivities of each material evaluated at Matsubara frequencies ($i\xi_n$, with n = 0, 1, 2, ...). However, this condition does not always guarantee repulsive forces, and furthermore, the dielectric function at *all* frequencies (essential for evaluation of Casimir forces) is known for a few solid and liquid materials. Potential strategies to fulfill the above inequation with materials already existing in nature include the modification of the dielectric function of one of the materials upon crystallization[36] or with hybrid systems comprising several materials such that the composite behaves as a homogeneous material with an effective dielectric function and density.[37−39] Additionally, when two interacting objects are under the influence of both Casimir and gravity forces, nanolevitation may take place if the Casimir force equals the gravity force at a certain (equilibrium) distance.[16,40] Nonetheless, intuition about the balance of such forces cannot be easily applied in systems containing real materials because the Casimir force will be determined by the multiple Fresnel coefficients and the dielectric permittivity of all materials composing the system, covering the UV and far-infrared ranges.

Received: November 27, 2014
Revised: February 17, 2015
Published: February 18, 2015

DOI: 10.1021/jp511851z
J. Phys. Chem. C 2015, 119, 5663−5670

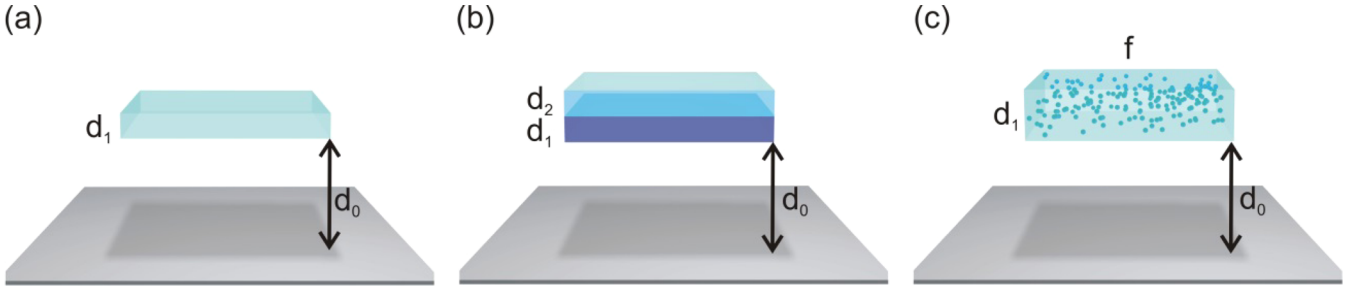

Figure 1. Schematics of the systems studied: (a) single layer with thickness d_1, immersed in a fluid at a separation distance, d_0, from the substrate; (b) bilayer with thickness d_2 for the top layer and d_1 for the bottom layer; and (c) matrix made up of one material of thickness d_1 with a volume fraction (f) of small inclusions of another material. The three systems are considered to have infinite area; i.e., the width and the length are much larger than the layer thickness.

Here, we investigate theoretically nanolevitation phenomena occurring in infinite (in area) plane-parallel systems in which a self-standing thin slab made of a real material immersed in a fluid stands over a substrate (see the three configurations here studied in the schematics in Figure 1). We will consider gap separations ≥50 nm, so instead of using the Hamaker approach that applies to distances shorter than a few nanometers,[41,42] we will consider the general Lifshitz formula that includes retardation effects of the field across the gap. In particular, we perform systematic analyses considering thin films of dielectric materials that can be easily processed and functionalized (thus avoiding the possible appearance of electrostatic forces), whose optical properties have been extensively studied in the literature (in particular, their dielectric functions), and with densities such that Casimir forces can finely cancel the gravity force when they are immersed in a fluid. Specifically, we consider thin films of Teflon, silica (SiO_2), and polystyrene (PS) immersed in glycerol, on top of a silicon (Si) substrate. We expect that functionalization strategies and the appearance of thin SiO_2 layers on top of the Si substrate will not strongly affect our results. We find that, while single layers of Teflon and SiO_2 present repulsive Casimir forces giving rise to stable equilibrium position, PS slabs display the opposite behavior. We predict nanolevitation phenomena also in hybrid systems whose components present Casimir forces and equilibrium distances of opposite nature (stable or unstable), in either a bilayer configuration or as a composite slab made of a homogeneous matrix with small inclusions inside. The results obtained for composite slabs are discussed in terms of the choice of the effective medium approximation considered. We show that the equilibrium distances are modified through the variation of the slab thickness in the single-layer configuration, the thickness of the individual components in the bilayer configuration, and the filling fraction of inclusions in the nanocomposites, parameters which have a strong effect on both Casimir and gravity forces.

2. THEORETICAL APPROACH

A schematic of a general multilayer system containing up to seven layers (m = 0, ±1, ±2, ±3) is displayed in Figure 2a. The medium mediating the Casimir interaction is denoted by "0", which in our studies will be a fluid. Positive and negative scripts account for materials (or layers) above or below the fluid, respectively. The thickness of each layer is indicated on the left, d_m, and the corresponding permittivities, $\varepsilon^{(m)}(i\xi_n)$, and densities, ρ_m, on the right. The Casimir force (per unit area) in such a multilayer system depends on the multiple Fresnel coefficients of the top ($R_j^{(+)}$) and bottom ($R_j^{(-)}$) surfaces of the

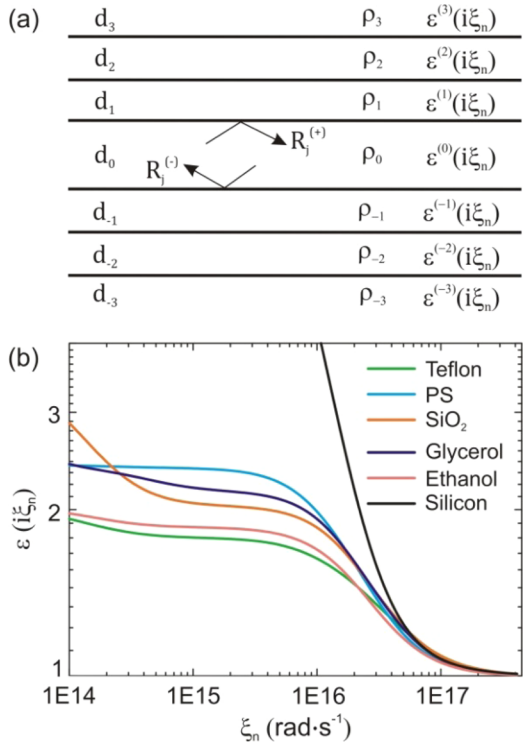

Figure 2. (a) Schematic of a multilayer system presenting the notation used to calculate the Casimir force. For each layer (m = 0, ±1, ±2, ±3), thickness is denoted by d_m, density by ρ_m, and dielectric functions at Matsubara frequencies by $\varepsilon^{(m)}(i\xi_n)$. (b) $\varepsilon(i\xi_n)$, for Teflon, PS, SiO_2, glycerol, ethanol, and Si (with a doping level 1.1 × 10^{15} cm^{-3} and resistivity 0.077 $(\Omega\cdot cm)^{-1}$). $\varepsilon(i\xi_n)$ for Si in an extended frequency range is shown in Figure S1 in the Supporting Information.

mediating layer, for transverse magnetic and electric polarizations (j = TM, TE, respectively) as[43]

$$F_c(d_0, T) = -\frac{k_B T}{\pi} \sum_{n=0}^{\infty'} \int_0^{\infty} k_n^{(0)} \mathbf{k}_\perp d\mathbf{k}_\perp \left\{ \left[\frac{e^{2k_n^{(0)} d_0}}{R_{TM}^{(+)} R_{TM}^{(-)}} - 1 \right]^{-1} + \left[\frac{e^{2k_n^{(0)} d_0}}{R_{TE}^{(+)} R_{TE}^{(-)}} - 1 \right]^{-1} \right\} \quad (1)$$

In the above expression, the wavevector inside the liquid layer is defined as $\mathbf{K} = (\mathbf{k}_\perp, k_n^{(0)})$; n = 0, 1, 2, ..., describes the discrete and infinite Matsubara frequencies $\xi_n = (2\pi k_B T n)/(\hbar)$; the "prime" in the summation indicates that the n = 0 term

DOI: 10.1021/jp511851z
J. Phys. Chem. C 2015, 119, 5663−5670

must be multiplied by a factor 1/2; and $R_j^{(\pm)}$ are the multiple Fresnel coefficients

$$R_j^{(\pm)}(n, \mathbf{k}_\perp) = \frac{r_j^{(0,\pm 1)} + \Gamma e^{-2k_n^{(\pm 1)} d_{\pm 1}}}{1 + r_j^{(0,\pm 1)} \Gamma e^{-2k_n^{(\pm 1)} d_{\pm 1}}} \tag{2}$$

In turn, $R_j^{(\pm)}$ are written in terms of the simple Fresnel formulas for each polarization, evaluated at the Matsubara frequencies, as

$$r_{\mathrm{TM}}^{(m,m')}(n, \mathbf{k}_\perp) = \frac{\varepsilon_n^{(m')} k_n^{(m)} - \varepsilon_n^{(m)} k_n^{(m')}}{\varepsilon_n^{(m')} k_n^{(m)} + \varepsilon_n^{(m)} k_n^{(m')}} \tag{3}$$

$$r_{\mathrm{TE}}^{(m,m')}(n, \mathbf{k}_\perp) = \frac{k_n^{(m)} - k_n^{(m')}}{k_n^{(m)} + k_n^{(m')}} \tag{4}$$

with

$$\Gamma = \frac{r_j^{(\pm 1,\pm 2)} + r_j^{(\pm 2,\pm 3)} e^{-2k_n^{(\pm 2)} d_{\pm 2}}}{1 + r_j^{(\pm 1,\pm 2)} r_j^{(\pm 2,\pm 3)} e^{-2k_n^{(\pm 2)} d_{\pm 2}}} \tag{5}$$

$$k_n^{(m)} = \left[\mathbf{k}_\perp^{\,2} + \varepsilon_n^{(m)} \frac{\xi_n^2}{c^2} \right]^{1/2} \tag{6}$$

Applying proper conditions to the number of layers and corresponding thickness to each single layer or bilayer configurations, we calculate the Casimir force mediated through medium (0).

The permittivity evaluated at Matsubara frequencies is obtained through eq 7

$$\varepsilon_n \equiv \varepsilon(i\xi_n) = 1 + \frac{2}{\pi} \int_0^\infty \frac{\omega \varepsilon''(\omega)}{\omega^2 + \xi_n^2} \mathrm{d}\omega \tag{7}$$

with $\varepsilon''(\omega)$ being the imaginary part of the dielectric function at ω frequencies, $\varepsilon(\omega) = \varepsilon'(\omega) + i\varepsilon''(\omega)$.

For SiO_2, PS, and Si (with a doping level 1.1×10^{15} cm^{-3} and resistivity 0.077 $(\Omega \cdot cm)^{-1}$) we consider the dielectric functions $\varepsilon(\omega)$ tabulated in ref 44, refs 45−47, and refs 10 and 48, respectively, and apply eq 7. For Teflon, ethanol, and glycerol, we employ oscillator models extracted from ref 14 which directly provide $\varepsilon(i\xi_n)$. On the other hand, for hybrid systems composed of two materials in the form of a matrix with a fraction of inclusions inside (f), we consider a single layer with an effective dielectric function, $\varepsilon_{\mathrm{eff}}(\omega)$,[39] and then apply eq 7. At least 12 mixing formulas have been proposed for calculating the effective permittivity[49] in hybrid systems, and the validity of some of the formulas applied to calculations of the Casimir force has been previously analyzed for polymer matrices with metallic inclusions inside.[39] However, the accuracy of the various theories can be judged only when comparing with experimental data.[50] In this work, we will use the widely employed Maxwell−Garnett ($\varepsilon_{\mathrm{eff}}^{\mathrm{MG}}(\omega)$) and Bruggeman ($\varepsilon_{\mathrm{eff}}^{\mathrm{Bru}}(\omega)$) models for spherical inclusions and compare them with results obtained using the Cuming ($\varepsilon_{\mathrm{eff}}^{\mathrm{Cum}}(\omega)$) model, which does not assume any special geometry for the inclusions, and it has been shown to be valid for large filling fractions.[49] The corresponding expressions for each model are the following

$$\varepsilon_{\mathrm{eff}}^{\mathrm{MG}}(\omega) = \varepsilon_{\mathrm{h}}(\omega) \frac{2(1-f)\varepsilon_{\mathrm{h}}(\omega) + (1+2f)\varepsilon_{\mathrm{i}}(\omega)}{(2+f)\varepsilon_{\mathrm{h}}(\omega) + (1-f)\varepsilon_{\mathrm{i}}(\omega)} \tag{8}$$

$$f \frac{\varepsilon_{\mathrm{i}}(\omega) - \varepsilon_{\mathrm{eff}}^{\mathrm{Bru}}(\omega)}{\varepsilon_{\mathrm{i}}(\omega) + 2\varepsilon_{\mathrm{eff}}^{\mathrm{Bru}}(\omega)} + (1-f) \frac{\varepsilon_{\mathrm{h}}(\omega) - \varepsilon_{\mathrm{eff}}^{\mathrm{Bru}}(\omega)}{\varepsilon_{\mathrm{h}}(\omega) + 2\varepsilon_{\mathrm{eff}}^{\mathrm{Bru}}(\omega)} = 0 \tag{9}$$

$$\log(\varepsilon_{\mathrm{eff}}^{\mathrm{Cum}}(\omega)) = f \log(\varepsilon_{\mathrm{i}}(\omega)) + (1-f)\log(\varepsilon_{\mathrm{h}}(\omega)) \tag{10}$$

with ε_{i} and ε_{h} being the dielectric functions of the inclusions and the host material, respectively.

For a given geometry at finite temperature and in a static situation, the nature (attractive or repulsive) and magnitude of the Casimir force depend on the dielectric response of all participating objects in the system and the separation distance. Figure 2b shows $\varepsilon(i\xi_n)$ for Teflon, PS, SiO_2, glycerol, ethanol, and Si. All materials considered in the figure satisfy the previous inequation at different frequency ranges in a configuration in which Si is taken as the substrate, glycerol or ethanol is the intermediate fluid, and the slab is made of any of the other materials. However, as we will show next, repulsive Casimir forces leading to stable equilibrium positions are found only for thin slabs made of Teflon and SiO_2 immersed in glycerol or if SiO_2 and PS materials are properly arranged in hybrid configurations. We also discarded for force calculations other liquids that, in comparison to SiO_2, PS, and Si in the same configuration, do not fulfill the previous inequation in any frequency range. Some of the tested liquids were water, methanol, pentane, hexane, heptane, octane, and some cycloalkanes.

3. RESULTS AND DISCUSSION

Single-Layer System. Let us first consider the case of a thin layer immersed in a fluid with materials that fulfill the inequation $\varepsilon^{(-1)}(i\xi_n) < \varepsilon^{(0)}(i\xi_n) < \varepsilon^{(1)}(i\xi_n)$. This is the simplest system that can be considered in which the dielectric permittivity of each material is well-defined, and the interaction is mediated through the simple Fresnel coefficients. Figure 3 shows the total force (per unit area) calculated using eq 1 at room temperature (T = 300 K) as a function of the separation distance, d_0, for thin films of (a) Teflon, (b) SiO_2, or (c) PS, immersed in glycerol over a Si substrate.

We consider experimentally available values of the film thicknesses,[51−53] d_1. In this configuration, and bearing in mind the original sign convention of F_0 ($F < 0$ attractive and $F > 0$ repulsive), the total force acting on the dielectric thin film is $F(d_0,T) = F_c(d_0,T) - F_g$, with $F_g = (\rho_1 - \rho_{\mathrm{glycerol}})gd_1$ and ρ_{Teflon} = 2.20 g/cm^3, $\rho_{\mathrm{SiO_2}}$ = 2.65 g/cm^3, ρ_{PS} = 1.05 g/cm^3, and ρ_{glycerol} = 1.26 g/cm^3, the corresponding densities. On one hand, systems consisting on single layers of Teflon and SiO_2 present a total repulsive (positive) force at short separation distances, which changes to be attractive (negative) at larger distances, tending to the asymptotic value of F_g for each slab thickness (i.e., F_c = 0). The distance at which the Casimir force compensates the gravity force ($F(d_{\mathrm{eq}})$ = 0) is a stable equilibrium distance; i.e., any slight deviation from that position will lead to a force pointing to the equilibrium position. On the other hand, for PS films immersed in glycerol the opposite behavior is found: a total attractive force governs at short distances, and a repulsive force is found at larger ones, due to the low density of PS. In this case, the equilibrium position is unstable since any deviation from it will provoke that the film will either get attached to the Si substrate (for $d_0 < d_{\mathrm{eq}}$) or float (for $d_0 > d_{\mathrm{eq}}$). In the paper, figures displaying results related to stable positions will be shown with solid lines and those related

DOI: 10.1021/jp511851z
J. Phys. Chem. C 2015, 119, 5663−5670

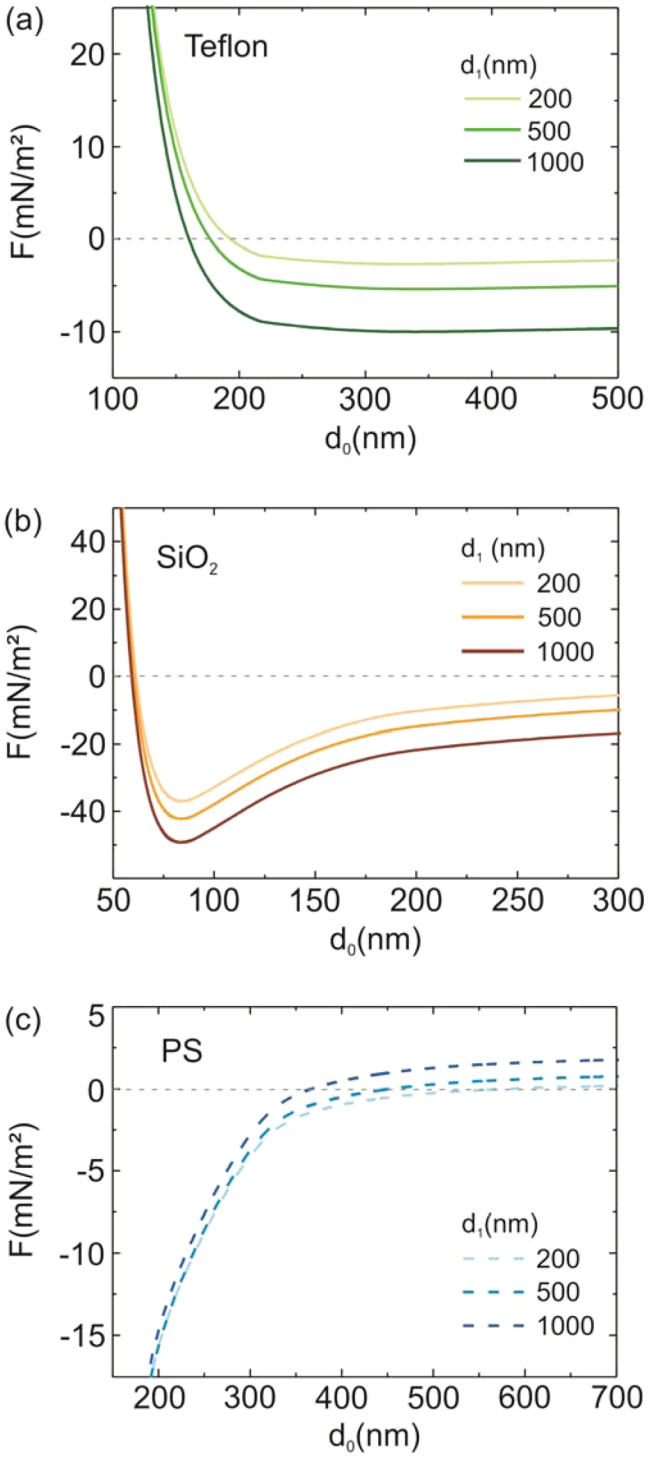

Figure 3. Total force acting on thin films of (a) Teflon, (b) SiO_2, and (c) PS immersed in glycerol over a Si substrate, as a function of the separation distance. Film thicknesses of d_1 =200, d_1 = 500, and d_1 = 1000 nm are considered. Solid lines correspond to systems displaying stable equilibrium positions and dashed lines to unstable ones. $F(d_0,T) = 0$ is marked with dashed gray lines.

to unstable positions with dashed lines. Isolated calculations of F_c as a function of the separation distance for SiO_2 and PS slabs are shown in Figure S2 in the Supporting Information. As the interaction between the bodies is established through fluctuating electromagnetic fields, and such fields are always present inside and extend beyond material boundaries,[54] the reach of the Casimir interaction will depend on the materials, slab thicknesses, and separation distances considered. In particular, it has been already shown that the strength of the Casimir force mainly depends on the slab thickness through contributions of TE and TM modes of the multiple Fresnel coefficients.[55] Eventually, the interaction between thick enough slabs must tend to the limiting case of two semi-infinite media separated a certain distance, and the interaction between slabs of a given thickness must be zero for large enough gap distances. Examples of the comparison between slabs of finite thickness and semi-infinite ones are provided in Figure S3 in the Supporting Information.

A similar system composed of PS thin slabs immersed in ethanol over a Si substrate was reported to display stable and unstable equilibrium distances under the influence of gravity.[56] However, the ethanol permittivity used in ref 56 seems to be inaccurate, as it has been already pointed out.[57] Calculations of the total force acting on such a system considering the proper permittivity of ethanol[14] show that no equilibrium positions are found (Figure S4 in the Supporting Information). Another phenomenon that may take place for a given system under the influence of both Casimir and gravity forces consists of the existence of both stable and unstable equilibrium positions. An example of this phenomenon is shown in Figure S5 in the Supporting Information.

For the three systems considered in Figure 3, we realized a deeper analysis of the stability of the equilibrium positions under thermal variations around room temperature. Figure 4 shows equilibrium distances as a function of the film thickness, d_1, for T = 250, 300, and 350 K. This analysis shows that equilibrium distances in systems with Teflon and SiO_2 present stable positions covering the range $d_{eq} \in [150, 215]$ nm and $d_{eq} \in [50,74]$ nm, respectively, with variations of ∼10% and 15% under temperature changes. Equilibrium positions also change with temperature for PS slabs but in this case with lighter variations of ∼5%, displaying unstable $d_{eq} \in [350, 770]$ nm. The temperature dependence of d_{eq} is explained through changes of the F_c in terms of the relative contributions of the TE and TM polarizations at $n = 0$ and $n > 0$ (eq 1). In all cases here considered, TE contributions hardly vary with temperature, concluding that TM modes are responsible for the variations found. A deeper analysis of TM contributions at $n = 0$ and $n > 0$ demonstrates that the higher the balance between both contributions, the smaller the variations of F_c with temperature and, therefore, of the equilibrium distances, as in the case of PS slabs. In contrast, for Teflon and SiO_2, a less balance between both contributions is found, leading to higher variations of d_{eq} with temperature (see Figure S6 in the Supporting Information).

We have seen that single layers of Teflon, SiO_2, and PS present equilibrium positions that can be tuned through the slab thickness. The question now is what happens when several materials are combined since it may have an effect on the Casimir force through either the multiple Fresnel coefficients (in multilayer systems) or the effective dielectric function (in composites), as well as on the gravity force through the density of all components. An interesting system to be analyzed is that composed of two materials which, in individual layers, present Casimir forces of different sign and equilibrium distances of opposite stability. In our studies we will focus on different mixtures of SiO_2 and PS, two materials that have been frequently combined,[58−64] whose optical properties are well-known, and with densities differing considerably.

DOI: 10.1021/jp511851z
J. Phys. Chem. C 2015, 119, 5663−5670

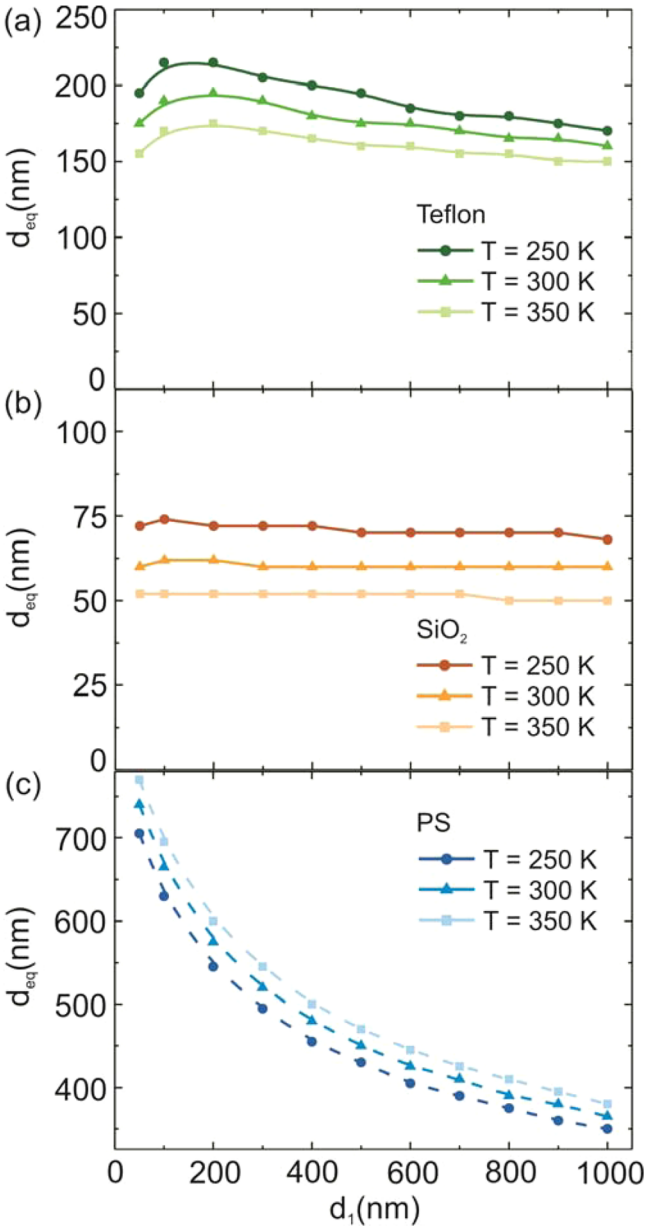

Figure 4. Equilibrium distance (d_{eq}) as a function of the slab thickness (d_1), at T = 250 K, T = 300 K, and T = 350 K for (a) Teflon, (b) SiO_2, and (c) PS, immersed in glycerol over a Si substrate. Solid lines correspond to stable equilibrium positions and dashed lines to unstable ones.

Bilayer System. One kind of hybrid system that can be fabricated is a bilayer film. As we will show next, the total force acting on such a system can be controlled at will through the layer thickness of the individual materials and the orientation of the bilayer with respect to the substrate (with either the SiO_2 or PS materials facing the substrate).

Figure 5 shows d_{eq} for a bilayer system immersed in glycerol over a Si substrate, as a function of (a) $d_1^{SiO_2}$ and (b) d_1^{PS}. Panel (a) corresponds to a configuration in which a thin layer of PS is on top of a SiO_2 slab, which in turn is facing the Si substrate, and panel (b) corresponds to the inverted configuration (see the schematics in the figure). The gravity force in this case is calculated as $F_g = g(\rho_1 d_1 + \rho_2 d_2 - \rho_{glycerol}(d_1 + d_2))$. We consider bottom thin films of $d_1 \in [40, 2000]$ nm and top films of $d_2 \in [10, 600]$ nm. For these slab thicknesses and materials,

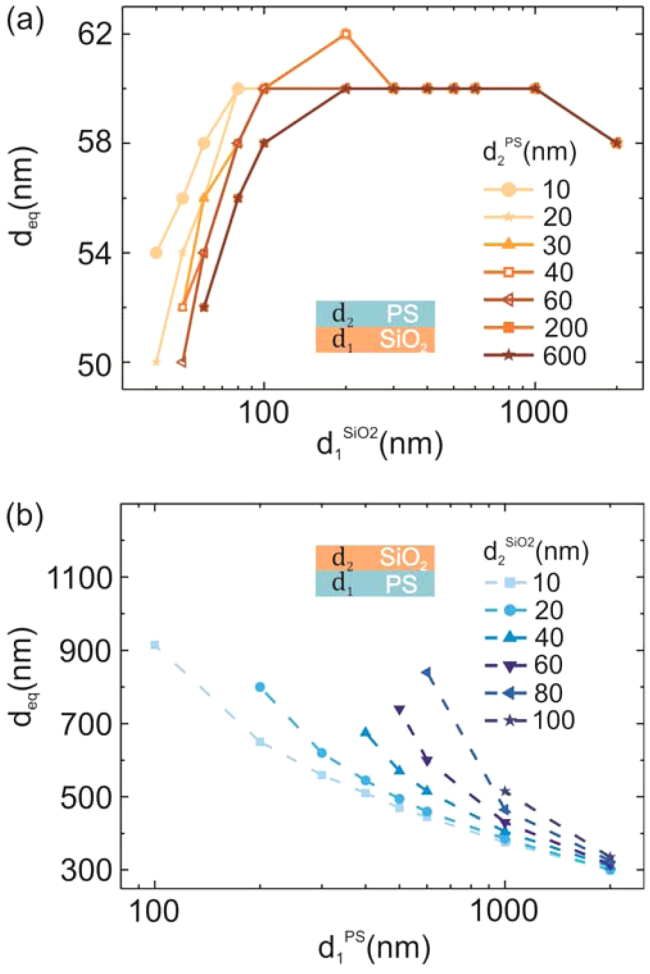

Figure 5. Equilibrium distance (d_{eq}) in a bilayer configuration (containing SiO_2 and PS), immersed in glycerol over a Si substrate, as a function of the slab thickness of the bottom layer (d_1), for different thicknesses of the top layer (d_2), for the configurations represented with schematics in each panel.

we find that d_{eq} can be tuned between 50 and 62 nm if SiO_2 is facing the substrate (Figure 5a) or between 300 and 915 nm if it is PS (Figure 5b). Due to the reach of the interaction between the bodies, for thin bottom films the Casimir force is strongly modified by the presence of the top material (i.e., Fresnel coefficients contain information on the layered system), changing the equilibrium distance remarkably. In contrast, for thick enough bottom layers ($d_1^{SiO_2} \sim 300$ nm and $d_1^{PS} \sim 2000$ nm), the Casimir interaction is the same as that of two semi-infinite substrates separated by a liquid, regardless of the thickness of the material on top (although it has an effect on the gravity force). Moreover, no equilibrium positions are found in panel (b) for bottom layers with $d_1^{PS} < 1000$ nm and top layers with $d_1^{SiO_2} > 100$ nm, as the low amount of PS cannot overcome attractive Casimir forces together with the weight of the SiO_2 film on top. Figures S7 and S8 in the Supporting Information display the Casimir, gravity, and total forces as a function of the separation distance for two limiting cases of thin and thick films in both configurations.

Composite System. Another appealing hybrid system amenable to the experimental realization consists of a matrix with a volume fraction of small inclusions inside[65] that will display a modified dielectric permittivity and, as a result, will have an effect on the Casimir force. In this case, the total force

DOI: 10.1021/jp511851z
J. Phys. Chem. C 2015, 119, 5663−5670

acting on the system can be tuned through the total thickness of the layer (d_1) and filling fraction of the inclusions (f). We consider two limiting cases of thin films (d_1 = 100 and 1000 nm), with 40% of PS inclusions (f = 0.4) inside a homogeneous matrix of SiO_2 and the complementary system, i.e., a PS matrix with 40% SiO_2 inclusions. For these hybrid systems, the gravity force is calculated as $F_g = g(f\rho_i d_1 + (1 - f)\rho_h d_1 - \rho_{glycerol} d_1)$, with i and h standing for inclusions and host, respectively. Figure 6a shows the total force acting on a SiO_2 matrix as a function of the separation distance, d_0, and using the effective permittivity provided by Maxwell–Garnett, Bruggeman, and Cuming models in eqs 8, 9, and 10. This strategy was previously considered in ref 39 to evaluate the effect on the Casimir force with polymer matrices with metallic inclusions inside. Results for the complementary system are displayed in Figure 6b, and $\varepsilon_{eff}(i\xi_n)$ for each model are shown in Figure S9 of the Supporting Information. Several trends are found for each model and configuration (panels (a) and (b)), as was previously indicated for metallic inclusions.[39] The three models follow the same trend, predicting stable d_{eq} in panel (a) but providing different distance values with maximum variations of ~30 nm, depending on the model considered. In contrast, in panel (b) no d_{eq} are obtained since a total force $F < 0$ for all separation distances is predicted by the Maxwell–Garnett model, while the Cuming and Bruggeman models produce stable positions. In all configurations and for all models predicting d_{eq}, the equilibrium distance is almost independent of the slab thickness (for the range of parameters here considered). Analysis of ε_{eff} ($i\xi_n$) in Figure S9 (Supporting Information) shows that both the Maxwell–Garnett and Bruggeman models provide an effective permittivity that tends to that of the host matrix depending on the f value, which nonetheless does not produce similar total forces. However, $\varepsilon_{eff}(i\xi_n)$ in the Cuming model hardly varies with f, and it is always less than that of the host matrix, which explains the predicted large repulsive Casimir forces and d_{eq}, in comparison to the other models. The relevance of the particular organization of the two materials in the hybrid film is reflected in the fact that the combination of the same materials at the same proportion in a bilayer, or in a composite configuration when nanolevitation is predicted, exhibits very different behavior. For instance, while a thin film (d_1 = 100 nm) of SiO_2 with 40% of PS inclusions presents stable equilibrium positions at $d_{eq} \in [97–128]$ nm (Figure 6a), a bilayer of 100 nm with 60 nm of SiO_2 facing the Si substrate, with a PS layer of 40 nm on top, finds the stable position at $d_{eq} \sim 54$ nm (Figure 5a), and the inverted configuration does not even present equilibrium positions (Figure 5b). The complementary system, a PS matrix with 40% of SiO_2 inclusions, presents $d_{eq} \in [19–137]$ nm (Figure 6b), while none of the corresponding bilayer configurations display equilibrium positions (Figure 5b).

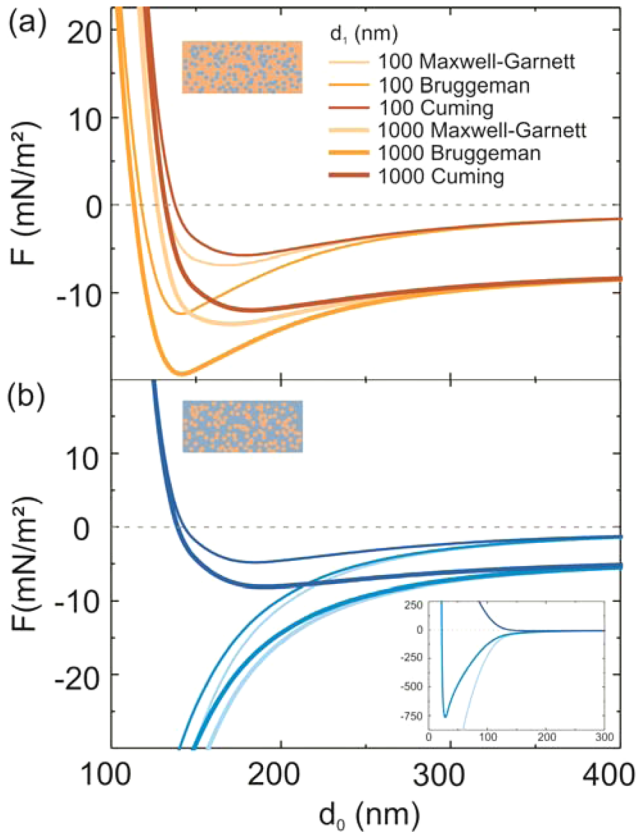

Figure 6. Total force (F) as a function of the separation distance (d_0), for (a) a SiO_2 matrix with 40% of PS inclusions (f = 0.4) and (b) the complementary system (PS matrix with 40% of SiO_2 inclusions), for d_1 = 100, 1000 nm, using the effective permittivity $\varepsilon_{eff}(i\xi_n)$ provided by Maxwell–Garnett, Bruggeman, and Cuming models in eqs 8, 9, and 10. $F(d_0,T) = 0$ is marked with dashed gray lines. Inset in panel (b) is a zoom-in close to short separation distances, showing $F = 0$ for both thicknesses of the Bruggeman model.

4. CONCLUSIONS

In conclusion, we have found a set of realistic materials and liquid compounds that give rise to nanolevitation in plane-parallel configurations due to the balance between gravity and Casimir forces. We have performed systematic studies in which those materials are analyzed as single layers or combined in bilayers or composites, all configurations providing tunable equilibrium distances of several tens and hundreds of nanometers. In particular, the equilibrium distances at which the Casimir force finely cancels the gravity force can be adjusted through the slab thickness in single-layer configurations. The Casimir force in bilayers can be tuned through the multiple Fresnel coefficients for thin enough layers (otherwise, the interaction is that of a single layer) and, therefore, through the thickness of each layer. For composites, the interaction is mediated through the simple Fresnel coefficients, and the choice of the model to represent the effective permittivity is critical since different models predict very different behavior. For those models predicting equilibrium distances, we show that the possibility to tune it lies now in the effective permittivity which can be modified through the filling fraction of the inclusions. Our results pave the way for novel suspension and nonadhesive strategies at the nanoscale.

■ ASSOCIATED CONTENT

Supporting Information

Additional calculations of the Casimir and gravity forces, separately, as well as the TE and TM contributions to the Casimir force and the effective permittivity of composite materials. This material is available free of charge via the Internet at http://pubs.acs.org.

■ AUTHOR INFORMATION

Corresponding Authors

*E-mail: sol.carretero@csic.es

DOI: 10.1021/jp511851z
J. Phys. Chem. C 2015, 119, 5663–5670

*E-mail: h.miguez@csic.es.

Author Contributions

The manuscript was written through contributions of all authors. All authors have given approval to the final version of the manuscript.

Notes

The authors declare no competing financial interest.

■ ACKNOWLEDGMENTS

The research leading to these results has received funding from the European Research Council under the European Union's Seventh Framework Programme (FP7/2007−2013)/ERC grant agreement n° 307081 (POLIGHT) and the Spanish Ministry of Economy and Competitiveness under grant MAT2011−23593. We thank Dr. G. Palasantzas for motivating discussions.

■ REFERENCES

(1) Dzyaloshinskii, I. E.; Lifshitz, E. M.; Pitaevskii, L. P. The general theory of van der Waals forces. *Adv. Phys.* **1961**, *10*, 165−209.
(2) Casimir, H. B. G. On the attraction between two perfectly conducting plates. *Proc. K. Ned. Akad. Wet.* **1948**, *51*, 793−796.
(3) Feiler, A. A.; Bergström, L.; Rutland, M. W. Superlubricity Using Repulsive van der Waals Forces. *Langmuir* **2008**, *24*, 2274−2276.
(4) Loskill, P.; Hähl, H.; Faidt, T.; Grandthyll, S.; Müller, F.; Jacobs, K. Is adhesion superficial? Silicon wafers as a model system to study van der Waals interactions. *Adv. Colloid Interface Sci.* **2012**, *179*, 107−113.
(5) Shahsavan, H.; Zhao, B. Conformal Adhesion Enhancement on Biomimetic Microstructured Surfaces. *Langmuir* **2011**, *27*, 7732−7742.
(6) Serry, F. M.; Walliser, D.; Maclay, G. J. The Anharmonic Casimir Oscillator (ACO) - the Casimir effect in a model microelectromechanical system. *J. Microelectromech. Syst.* **1995**, *4*, 193−205.
(7) Chan, H. B.; Aksyuk, V. A.; Kleiman, R. N.; Bishop, D. J.; Capasso, F. Quantum Mechanical Actuation of Microelectromechanical Systems by the Casimir Force. *Science* **2001**, *291*, 1941.
(8) Lifshitz, E. M. The theory of molecular attractive forces between solids. *Sov. Phys. JETP* **1956**, *2*, 73.
(9) Palasantzas, G.; van Zwol, P. J.; De Hosson, J.; Th, M. Transition from Casimir to van der Waals force between macroscopic bodies. *Appl. Phys. Lett.* **2008**, *93*, 121912.
(10) Duraffourg, L.; Andreucci, P. Casimir force between doped silicon slabs. *Phys. Lett. A* **2006**, *359*, 406−411.
(11) Svetovoy, V. B.; van Zwol, P. J.; Palasantzas, G.; De Hosson, J.; Th, M. Optical properties of gold films and the Casimir force. *Phys. Rev. B* **2008**, *77*, 035439.
(12) Klimchitskaya, G. L.; Mohideen, U.; Mostepanenko, V. M. The Casimir force between real materials: Experiment and theory. *Rev. Mod. Phys.* **2009**, *81*, 1827.
(13) Broer, W.; Palasantzas, G.; Knoester, J.; Svetovoy, V. B. Roughness correction to the Casimir force at short separations: Contact distance and extreme value statistics. *Phys. Rev. B* **2012**, *85*, 155410.
(14) van Zwol, P. J.; Palasantzas, G. Repulsive Casimir forces between solid materials with high-refractive-index intervening liquids. *Phys. Rev. A* **2010**, *81*, 062502.
(15) Genet, C.; Lambrecht, A.; Reynaud, S. Casimir force and the quantum theory of lossy optical cavities. *Phys. Rev. A* **2003**, *67*, 043811.
(16) Rodriguez, A. W.; McCauley, A. P.; Woolf, D.; Capasso, F.; Joannopoulos, J. D.; Johnson, S. G. Nontouching Nanoparticle Diclusters Bound by Repulsive and Attractive Casimir Forces. *Phys. Rev. Lett.* **2010**, *104*, 160402.
(17) Esquivel-Sirvent, R.; Villarreal, C. Superlattice-mediated tuning of Casimir forces. *Phys. Rev. A* **2001**, *64*, 052108.
(18) Raabe, C.; Knöll, L.; Welsch, D. G. Three-dimensional Casimir force between absorbing multilayer dielectrics. *Phys. Rev. A* **2003**, *68*, 033810.
(19) Zhao, R.; Koschny, Th.; Economou, E. N.; Soukoulis, C. M. Repulsive Casimir forces with finite-thickness slabs. *Phys. Rev. B* **2011**, *83*, 075108.
(20) Bao, Y.; Guérout, R.; Lussange, J.; Lambrecht, A.; Cirelli, R. A.; Klemens, F.; Mansfield, W. M.; Pai, C. S.; Chan, H. B. Casimir Force on a Surface with Shallow Nanoscale Corrugations: Geometry and Finite Conductivity Effects. *Phys. Rev. Lett.* **2010**, *105*, 250402.
(21) Rodriguez, A. W.; Capasso, F.; Johnson, S. G. The Casimir effect in microstructured geometries. *Nat. Photonics* **2011**, *5*, 211−221.
(22) Haro, J.; Elizalde, E. Hamiltonian Approach to the Dynamical Casimir Effect. *Phys. Rev. Lett.* **2006**, *97*, 130401.
(23) Kats, E. I. Van der Waals Forces in Non-Isotropic Systems. *Sov. Phys. JETP* **1971**, *33*, 634−636.
(24) Parsegian, V. A.; Weiss, G. H. Dielectric Anisotropy and the Van der Waals Interaction between Bulk Media. *J. Adhes.* **1972**, *3*, 259−267.
(25) Esquivel-Sirvent, R.; Schatz, G. C. Van der Waals Torque Coupling between Slabs Composed of Planar Arrays of Nanoparticles. *J. Phys. Chem. C* **2013**, *117*, 5492−5496.
(26) Antezza, M.; Pitaevskii, L. P.; Stringari, S.; Svetovoy, V. B. Casimir-Lifshitz force out of thermal equilibrium. *Phys. Rev. A* **2008**, *77*, 022901.
(27) Milton, K. A. The Casimir effect: recent controversies and progress. *J. Phys. A* **2004**, *37*, R209.
(28) Munday, J. N.; Capasso, F.; Parsegian, V. A. Measured long-range repulsive Casimir-Lifshitz forces. *Nature* **2009**, *457*, 170−173.
(29) Hoye, J. S.; Brevik, I.; Aarseth, J. B.; Milton, K. A. What is the Temperature Dependence of the Casimir Effect? *J. Phys. A* **2006**, *39*, 6031−38.
(30) Lamoreaux, S. K. The Casimir force: background, experiments, and applications. *Rep. Prog. Phys.* **2005**, *68*, 201.
(31) Bostrom, M.; Sernelius, B. E. Thermal Effects on the Casimir Force in the 0.1− 5μm Range. *Phys. Rev. Lett.* **2000**, *84*, 4757.
(32) Bordag, M.; Geyer, B.; Klimchitskaya, G. L.; Mostepanenko, V. M. Casimir Force at Both Nonzero Temperature and Finite Conductivity. *Phys. Rev. Lett.* **2000**, *85*, 503.
(33) Bentsen, V. S.; Herikstad, R.; Skriudalen, S.; Brevik, I.; Hoye, J. S. Calculation of the Casimir Force between Similar and Dissimilar Metal Plates at Finite Temperature. *J. Phys. A* **2005**, *38*, 9575.
(34) Yampol'skii, V. A.; Savel'ev, S.; Mayselis, Z. A.; Apostolov, S. S.; Nori, F. Anomalous temperature dependence of the Casimir force for thin metal films. *Phys. Rev. Lett.* **2008**, *101*, 096803.
(35) Obrecht, J. M.; Wild, R. J.; Antezza, M.; Pitaevskii, L. P.; Stringari, S.; Cornell, E. A. Measurement of the Temperature Dependence of the Casimir-Polder Force. *Phys. Rev. Lett.* **2007**, *98*, 063201.
(36) Torricelli, G.; van Zwol, P. J.; Shpak, O.; Palasantzas, G.; Svetovoy, V. B.; Binns, C.; Kooi, B. J.; Jost, P.; Wuttig, M. Casimir Force Contrast Between Amorphous and Crystalline Phases of AIST. *Adv. Funct. Mater.* **2012**, *22*, 3729−3736.
(37) Galkina, E. G.; Ivanov, B. A.; Savelev, S.; Yampolskii, V. A.; Nori, F. Drastic change of the Casimir force at the metal-insulator transition. *Phys. Rev. B* **2009**, *80*, 125119.
(38) Esquivel-Sirvent, R. Reduction of the Casimir force using aerogels. *J. Appl. Phys.* **2007**, *102*, 034307.
(39) Esquivel-Sirvent, R.; Schatz, G. C. Mixing rules and the Casimir force between composite systems. *Phys. Rev. A* **2011**, *83*, 042512.
(40) Rodriguez, A. W.; Munday, J.; Davlit, D.; Capasso, F.; Joannopoulos, J. D.; Johnson, S. G. Stable suspension and dispersion-induced transitions from repulsive Casimir forces between fluid-separated eccentric cylinders. *Phys. Rev. Lett.* **2008**, *101*, 190404.
(41) French, R. H. Origins and Applications of London Dispersion Forces and Hamaker Constants in Ceramics. *J. Am. Ceram. Soc.* **2000**, *83*, 2117−46.
(42) Walker, D. A.; Kowalczyk, B.; Olvera de la Cruz, M.; Grzybowski, B. A. Electrostatics at the nanoscale. *Nanoscale* **2011**, *3*, 1316−1344.

DOI: 10.1021/jp511851z
J. Phys. Chem. C 2015, 119, 5663−5670

(43) Bordag, M.; Klimchitskaya, G. L.; Mohideen, U.; Mostepanenko, V. M. *Advances in the Casimir Effect*; Oxford University Press: U.K., 2009.
(44) Kitamura, R.; Pilon, L.; Jonasz, M. Optical constants of silica glass from extreme ultraviolet to far infrared at near room temperature. *Appl. Opt.* **2007**, *46*, 8118.
(45) Strom, U.; Hendrickson, J. R.; Wagner, Ri.; Taylor, P. C. Disorder-induced far infrared absorption in amorphous materials. *Solid State Commun.* **1974**, *15*, 1871−1875.
(46) Folks, W. R.; Pandey, S. K.; Pribil, G.; Slafer, D.; Manning, M.; Boreman, G. Reflective infrared ellipsometry of plastic films. *Int. J. Infrared Milli. Waves* **2006**, *27*, 1553−1571.
(47) Inagaki, T.; Arakawa, E. T.; Hamm, R. N.; Williams, M. W. Optical properties of polystyrene from the near-infrared to the x-ray region and convergence of optical sum rules. *Phys. Rev. B* **1977**, *15*, 6.
(48) Edwards, D. F. In *Handbook of Optical Constant of Solid*, 2nd ed.; Palik, E. D., Ed.; Academic Press: New York, 1985; Vol. *1*, p 547.
(49) Prasad, A.; Prasad, K. Effective permittivity of random composite media: Acomparative study. *Phys. B* **2007**, *137*, 396−432.
(50) Granqvist, C. G.; Hunderi, O. Optical properties of Ag-SiO_2 Cermet films: A comparison of effective-medium theories. *Phys. Rev. B* **1978**, *18*, 2897.
(51) Huang, J.; Juszkiewicz, M.; de Jeu, W. H.; Cerda, E.; Emrick, T.; Menon, N.; Russell, T. P. Capillary Wrinkling of Floating Thin Polymer Films. *Science* **2007**, *3,17* (5838), 650−653.
(52) Maekawa, S.; Okude, K.; Ohishi, T. Synthesis of SiO2 thin films by sol-gel method using photoirradiation and molecular structure analysis. *J. Sol-Gel Sci. Technol.* **1994**, *2*, 497.
(53) Maekawa, S.; Okude, K.; Ohishi, T. Synthesis, properties, and molecular structure analysis of SiO_2 thin films prepared by Sol-Gel method. Electron. *Commun. Jpn. Part II* **1994**, *77*, 86−92.
(54) Svetovoy, V. B.; Palasantzas, G. Influence of surface roughness on dispersion forces. *Adv. Colloid Interface Sci.* **2015**, *216*, 1−19.
(55) Inui, N. Thickness dependence of the Casimir force between a magnetodielectric plate and a diamagnetic plate. *Phys. Rev. A* **2001**, *84*, 052505.
(56) Rodriguez, A. W.; Woolf, D.; McCauley, A. P.; Capasso, F.; Joannopoulos, J. D.; Johnson, S. G. Achieving a Strongly Temperature-Dependent Casimir Effect. *Phys. Rev. Lett.* **2010**, *105*, 060401.
(57) van Zwol, P. J.; Palasantzas, G.; De Hosson, J.; Th, M. Influence of dielectric properties on van der Waals/Casimir forces in solid-liquid systems. *Phys. Rev. B* **2009**, *79*, 195428.
(58) Calvo, M.; Sobrado, O.; Lozano, G.; Miguez, H. Molding with nanoparticle-based one-dimensional photonic crystals: a route to flexible and transferable Bragg mirrors of high dielectric contrast. *J. Mater. Chem.* **2009**, *19* (20), 3144−3148.
(59) Calvo, M. E.; Castro Smirnov, J. R.; Miguez, H. Novel approaches to flexible visible transparent hybrid films for ultraviolet protection. *J. Polym. Sci., Part B: Polym. Phys.* **2012**, *50* (14), 945−956.
(60) Druffel, T.; Mandzy, N.; Sunkara, M.; Grulke, E. Polymer nanocomposite thin film mirror for the infrared region. *Small* **2008**, *4* (4), 459−461.
(61) DeCorby, R. G.; Ponnampalam, N.; Nguyen, H. T.; Clement, T. J. Robust and Flexible Free-Standing All-Dielectric Omnidirectional Reflectors. *Adv. Mater.* **2007**, *19*, 193−196.
(62) Bourgeat-Lami, E.; Lang, J. Encapsulation of Inorganic Particles by Dispersion Polymerization in Polar Media: 1. Silica Nanoparticles Encapsulated by Polystyrene. *J. Colloid Interface Sci.* **1998**, *197* (2), 293−308.
(63) Tiarks, F.; Landfester, K.; Antonietti, M. Silica nanoparticles as surfactants and fillers for latexes made by miniemulsion polymerization. *Langmuir* **2001**, *17* (19), 5775−5780.
(64) Ding, X.; Zhao, J.; Liu, Y.; Zhang, H.; Wang, Z. Silica nanoparticles encapsulated by polystyrene via surface grafting and in situ emulsion polymerization. *Mater. Lett.* **2004**, *58* (25), 3126−3130.
(65) Yang, H.; Coombs, N.; Ozin, G. A. Thickness control and defects in oriented mesoporous silica films. *J. Mater. Chem.* **1998**, *8*, 1205−1211.

DOI: 10.1021/jp511851z
J. Phys. Chem. C 2015, 119, 5663−5670